

NIH RELAIS Document Delivery

NIH-10286769

JEFFDUYN

NIH -- W1 J0748DEL

JOZEF DUYN
10 Center Dirve
Bldg. 10/Rm.1L07
Bethesda, MD 20892-1150

ATTN:	SUBMITTED: 2002-08-29 17:22:16
PHONE: 301-594-7305	PRINTED: 2002-09-03 12:12:12
FAX: -	REQUEST NO.:NIH-10286769
E-MAIL:	SENT VIA: LOAN DOC 7967406

NIH	Fiche to Paper	Journal
TITLE:	JOURNAL OF MAGNETIC RESONANCE IMAGING : JMRI	
PUBLISHER/PLACE:	Wiley, New York, NY :	
VOLUME/ISSUE/PAGES:	1997 Mar-Apr;7(2):371-5	371-5
DATE:	1997	
AUTHOR OF ARTICLE:	Yang Y; Mattay VS; Weinberger DR; Frank JA; Duyn JH	
TITLE OF ARTICLE:	Localized echo-volume imaging methods for function	
ISSN:	1053-1807	
OTHER NOS/LETTERS:	Library reports holding volume or year 9105850 9090593	
SOURCE:	PubMed	
CALL NUMBER:	W1 J0748DEL	
REQUESTER INFO:	JEFFDUYN	
DELIVERY:	E-mail: jhd@helix.nih.gov	
REPLY:	Mail:	

NOTICE: THIS MATERIAL MAY BE PROTECTED BY COPYRIGHT LAW (TITLE 17, U.S. CODE)

---National-Institutes-of-Health,-Bethesda,-MD-----

Localized Echo-Volume Imaging Methods for Functional MRI

Yihong Yang, PhD • Venkata S. Mattay, MD • Daniel R. Weinberger, MD • Joseph A. Frank, MD
Jeff H. Duyn, PhD

To perform true three-dimensional activation experiments in the human brain, dedicated localized echo-volume imaging (L-EVI) methods were developed. Three-dimensional acquisition allows generation of activation maps with minimal vascular enhancement related to inflow effects. The rapid acquisition of the L-EVI (~100 msec) reduces signal instabilities caused by motion, facilitating the detection of the small intensity changes expected with brain activation. Single-shot L-EVI was performed on normal volunteers at 1.5 T, imaging a three-dimensional predefined volume ($240 \times 45 \times 45 \text{ mm}^3$) in the superior portion of the brain with a spatial resolution of $3.75 \times 5 \times 5 \text{ mm}^3$. Increased brain coverage was achieved with a multi-volume imaging (three-shot) version, which simultaneously achieved effective suppression of signals from cerebrospinal fluid. In addition, both asymmetric spin-echo (ASE) and spin-echo (SE) versions of the technique were used to detect blood oxygenation level dependent (BOLD) signal changes in the motor cortex with a finger-tapping paradigm. Images obtained by the L-EVI sequence were qualitatively comparable to standard multislice two-dimensional echo-planar images. Both ASE and SE functional MRI (fMRI) experiments showed consistent activation in the contralateral primary sensorimotor cortex. Furthermore, significant differences in location and magnitude of activation was observed between the two methods, confirming theoretical predictions.

Index terms: fMRI • Echo volume imaging • Motor cortex • BOLD • EPI

JMRI 1997; 7:371-375

Abbreviations: ASE = asymmetric spin echo, BOLD = blood oxygenation level dependent, CSF = cerebrospinal fluid, EPI = echo-planar imaging, EVI = echo-volume imaging, FLASH = fast low angle shot, fMRI = functional MRI, FOV = field of view, L-EVI = localized echo-volume imaging, PSM = primary sensorimotor cortex, RF = radiofrequency, SE = spin echo, TOF = time of flight.

From the Laboratory of Diagnostic Radiology Research, OIR (Y.Y., J.A.F., J.H.D.), and Clinical Brain Disorders Branch, NIMH (V.S.M., D.R.W.), National Institutes of Health, Building 10, Room B1N-256, Bethesda, MD 20892. Received July 9, 1996; revision requested September 19; revision received September 26; accepted October 7. Presented at 4th annual scientific meeting of the International Society for Magnetic Resonance in Medicine, New York, 1996. Address reprint requests to J.H.D.

© ISMRM, 1997

FUNCTIONAL MRI (fMRI) based on blood oxygenation level dependent (BOLD) contrast provides a noninvasive tool for the study of human brain function (1,2). Among the techniques used for BOLD fMRI, echo-planar imaging (EPI) (3) has been particularly successful (4-6) and has demonstrated the ability to discriminate small activation-related signal changes from background noise. An important reason for this success is that EPI collects an entire two-dimensional scan in a single shot (~100 msec) and, therefore, is relatively insensitive to signal instabilities caused by physiologic fluctuations, related to cardiac and respiratory cycles. However, most EPI studies have used two-dimensional slice acquisitions (6). A potential problem of slice acquisition methods in fMRI is the artificial enhancement from inflowing spins, which could generate relatively large activation-related signal changes in regions such as draining veins (7-10). This can be a significant effect when measurements are made under saturating conditions, for example, in experiments with short TRs and large flip angles. However, this effect could be reduced by performing a true three-dimensional acquisition (11).

An extension of EPI to single-shot three-dimensional techniques, also known as echo-volume imaging (EVI), was first introduced by Mansfield et al (12) and was later applied to human brain imaging (13). Recently, preliminary results of EVI activation studies were presented (14). These studies demonstrated the capability of the method to scan large brain volumes but had severely limited resolution because of signal decay during data acquisition due to T2* effects. The spatial resolution could be markedly improved by zooming in to a localized volume, as can be done in localized EVI (L-EVI) (12). In this study, L-EVI is applied to activation studies of the human motor cortex, scanning a predefined volume with a nominal spatial resolution of $3.75 \times 5 \times 5 \text{ mm}^3$.

• MATERIALS AND METHODS

The pulse scheme for the L-EVI sequence is shown in Figure 1a. A column ($240 \times 45 \times 45 \text{ mm}^3$ with long axis in the x direction) was selected by a spin-echo (SE) radiofrequency (RF) sequence, in combination with slice-selection gradients in two orthogonal directions (y and z). The RF pulses were Gaussian apodized sinc waveforms with two sidelobes each. Frequency encodings were applied in the x direction by an alternating readout gradient. Sixty-four data points were acquired during each frequency encoding with a field of view (FOV) of 240 mm. A 10×10

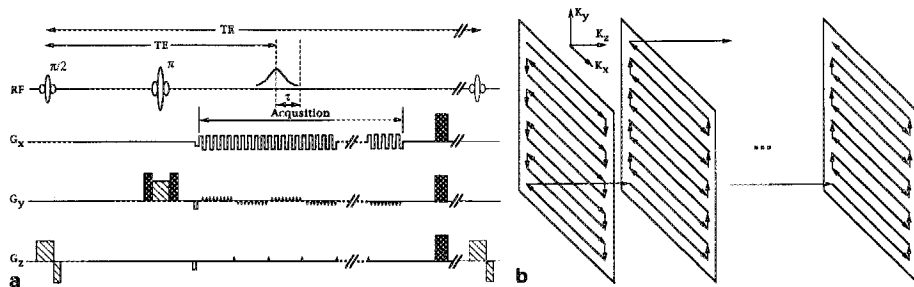


Figure 1. (a) Pulse sequence for the L-EVI acquisition, indicating RF pulses and gradient schemes. (b) The k-space trajectory of the L-EVI sequence.

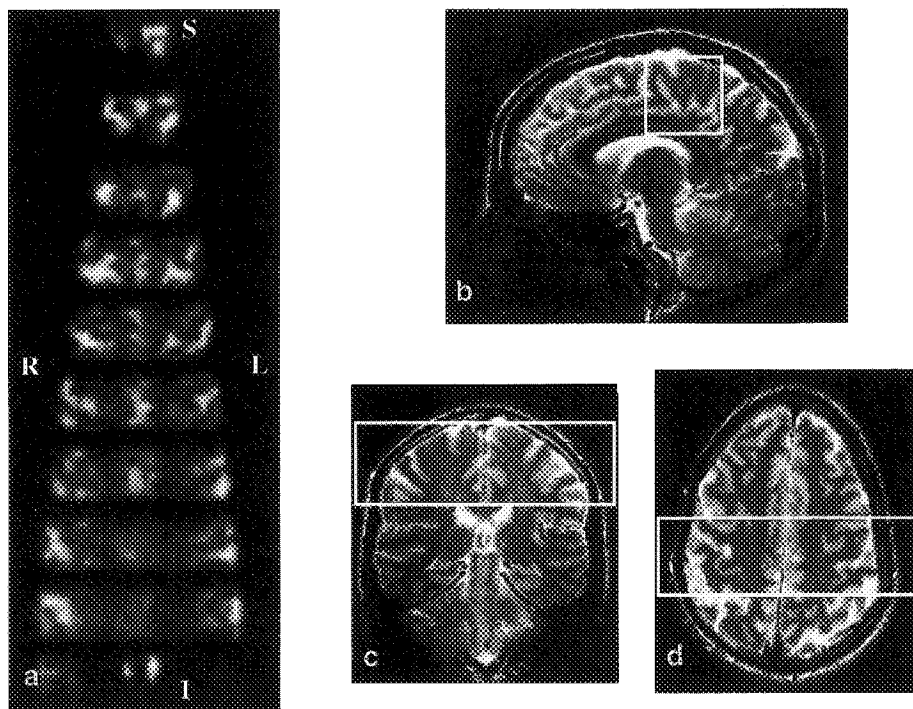


Figure 2. (a) Image of a selected column in the superior portion of the brain acquired with the L-EVI sequence (TE = 30 msec, $\tau = 30$ msec), displayed in axial slices. (b, c, d) Sagittal, coronal, and axial anatomical images of the brain, respectively, indicating the location of the selected column.

phase-encoding scheme was applied in y and z directions using gradient "blips." The FOV in the y and z direction was 50 mm to render 5-mm resolution in the two directions. The k-space trajectory generated by the gradient scheme is shown in Figure 1b. A data set without gradient blips was collected and used for phase correction. Asymmetric SE signals were acquired by offsetting the relative positions of the data acquisition window and calculated SE position by a time τ . Full k-space data were acquired in both SE and asymmetric SE (ASE) scans, but T2* weighting was different in the two scans. Multiple volume imaging, similar to multiple slice imaging in conventional EPI, can be performed by shifting the frequency of either the $\pi/2$ or the π RF pulse.

Experiments were performed on a 1.5-T SIGNA scanner (General Electric Medical Systems, Milwaukee, WI) equipped with an insertable gradient/RF coil assembly (Medical Advances, Milwaukee, WI) with maximum strength of $20 \text{ mT}\cdot\text{m}^{-1}$ and maximum slew rate of $100 \text{ T}\cdot\text{m}^{-1}\cdot\text{s}^{-1}$.

Anatomical scans and functional imaging data were acquired from six normal subjects. Guided by anatomical images, a column ($240 \times 45 \times 45 \text{ mm}^3$, long axis in left-right direction) was selected in the superior portion of the brain covering the primary sensorimotor cortex. Shimming was performed carefully on the selected volume to minimize distortion in the L-EVI images related to B_0 field in-

homogeneity. SE and ASE functional data sets were collected to compare the sensitivity to T2 and T2* weighting, respectively. TE and TR were 90 msec and 2 seconds, respectively, for both the SE and ASE sequence, and offset time (τ) for the ASE sequence was 30 msec. In each data set, 120 volume scans were acquired in 4 minutes, during which the subject switched between rest and finger tapping every 30 seconds (four "off-states" and four "on-states"). The finger tapping was self-paced (~ 2 Hz) and consisted of sequential thumb-to-digit opposition with the dominant hand. Ear plugs were used to reduce noise, and foam packs were applied to restrict head motion.

To investigate the approximate location and size of the larger vascular structures, high-resolution (512×512 with FOV $240 \times 240 \text{ mm}^2$) two-dimensional multislice time-of-flight (TOF) axial images (five slices, 5 mm in thickness) of the motor cortex region were acquired with a spoiled gradient-echo sequence (TE/TR = 10/60 msec, flip angle = 50°). The TOF images were acquired corresponding to the central five slices of the L-EVI image in the axial direction and were used to indicate voxels in the EVI data set with possible vascular contributions. Registration of the EVI data to the TOF images was performed by alignment of the central and precentral sulci. Detailed anatomical structures of the brain, including the gray and white matter and blood vessels, were clearly visible on the TOF images.

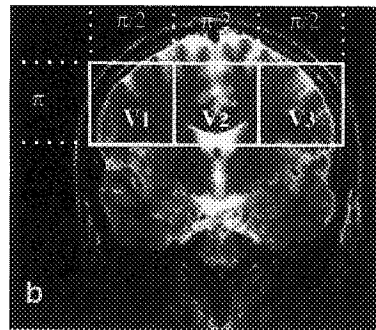
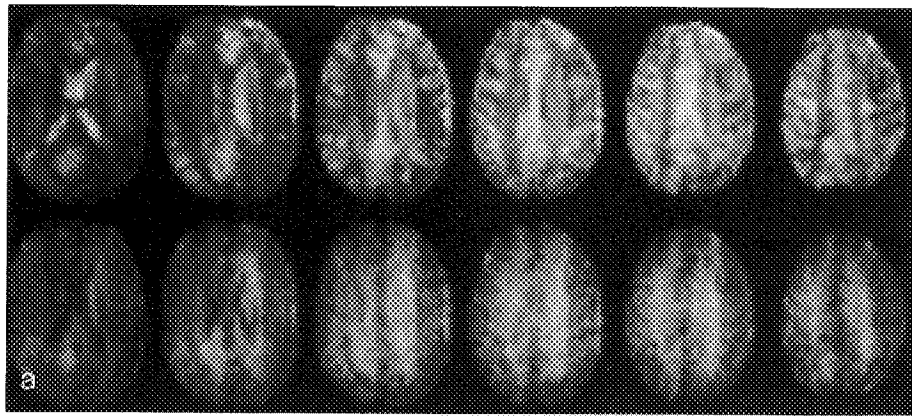


Figure 3. (a) Axial images of a slab (central six slices) in the superior brain acquired with the multiple-column (three columns) L-EVI sequence (top row, TE/TR = 30/4,000 msec, $\tau = 30$ msec), and with CSF nulling in the steady state (bottom row, TE/TR = 30/1,400 msec, $\tau = 30$ msec). (b) Coronal anatomical image of the brain indicating the location of the three selected columns.

Data were processed off line on a Sun-SPARC workstation (Sun Microsystems, Mountain View, CA). For the L-EVI data, phase errors were corrected by a reference data set acquired without gradient blips. The 120 volume images were registered to the first image to correct for rigid body motion between scans. The registration routine was based on a custom written software package using a multiresolution least-squares difference algorithm with cubic spline interpolation (15,16).

The time courses of the functional data were then analyzed, voxel by voxel, using a Student *t* test to identify voxels with significantly different signal changes between the "on" and "off" states (17). A noise threshold for excluding voxels outside the brain was estimated from a histogram of the signal intensities of all voxels, and voxels with signal intensities below the threshold were excluded. A statistical threshold was established by the Student *t* test adjusted for the total number of cortical voxels using an unbiased Bonferroni correction (18,19). The Bonferroni correction α level was determined for each individual data set. Because brain cortex represents approximately 50 to 60% of the total brain volume (20), the total number of cortical voxels in the brain column was typically 1,000 (55% of ~1,800 voxels in the selected brain region), resulting in an α level of 2.5×10^{-5} per voxel. The corresponding Student *t* cutoff (one-sided probability of .025) was approximately 4.20 (slightly varying from subject to subject) and voxels with *t* score above the threshold were considered as significantly "activated." The activation maps were scaled and overlaid on the TOF images for further examination.

• RESULTS

The images obtained by the L-EVI sequence were qualitatively comparable to the standard EPI images with similar experimental parameters. A typical single-shot ASE-EVI data set from a column in the superior portion of the brain is shown in Figure 2a (displayed in axial

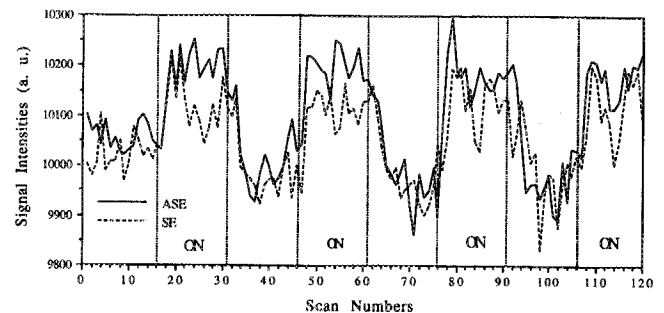


Figure 4. Examples of signal intensity time courses in the activated motor cortex regions for the ASE (solid line) and SE (dashed line) studies. A finger-tapping task with alternative "rest (off)" and "active (on)" states was performed in each study. Note that the signal increases during the "on" states in the ASE studies are larger than that in the SE studies.

slices). The data was acquired in a total time of 100 msec. The location of the column is indicated in three orthogonal anatomical images in Figures 2b through 2d.

Multiple volume images can be obtained if larger brain volumes are desired. As an example, Figure 3a shows a three-column ASE-EVI image covering a 45-mm-thick axial slab of the superior brain (top row, TR = 4 seconds). The locations of the three columns are indicated in a coronal image in Figure 3b. Notice that at TRs on the order of T1, potential problems arise due to regional saturation. In multiple volume imaging, this effect can be exploited to perform cerebrospinal fluid (CSF) nulling. As in standard (single-volume) EVI, volume selection is performed by the slice-selective $\pi/2$ and π RF pulses. Because in the multivolume experiments all volumes share the slice excited by the π RF pulses (Fig. 3b), CSF nulling can be performed by using the π RF pulse as both the refocusing pulse of the current volume (eg, V_1 in Fig. 3b), as well as

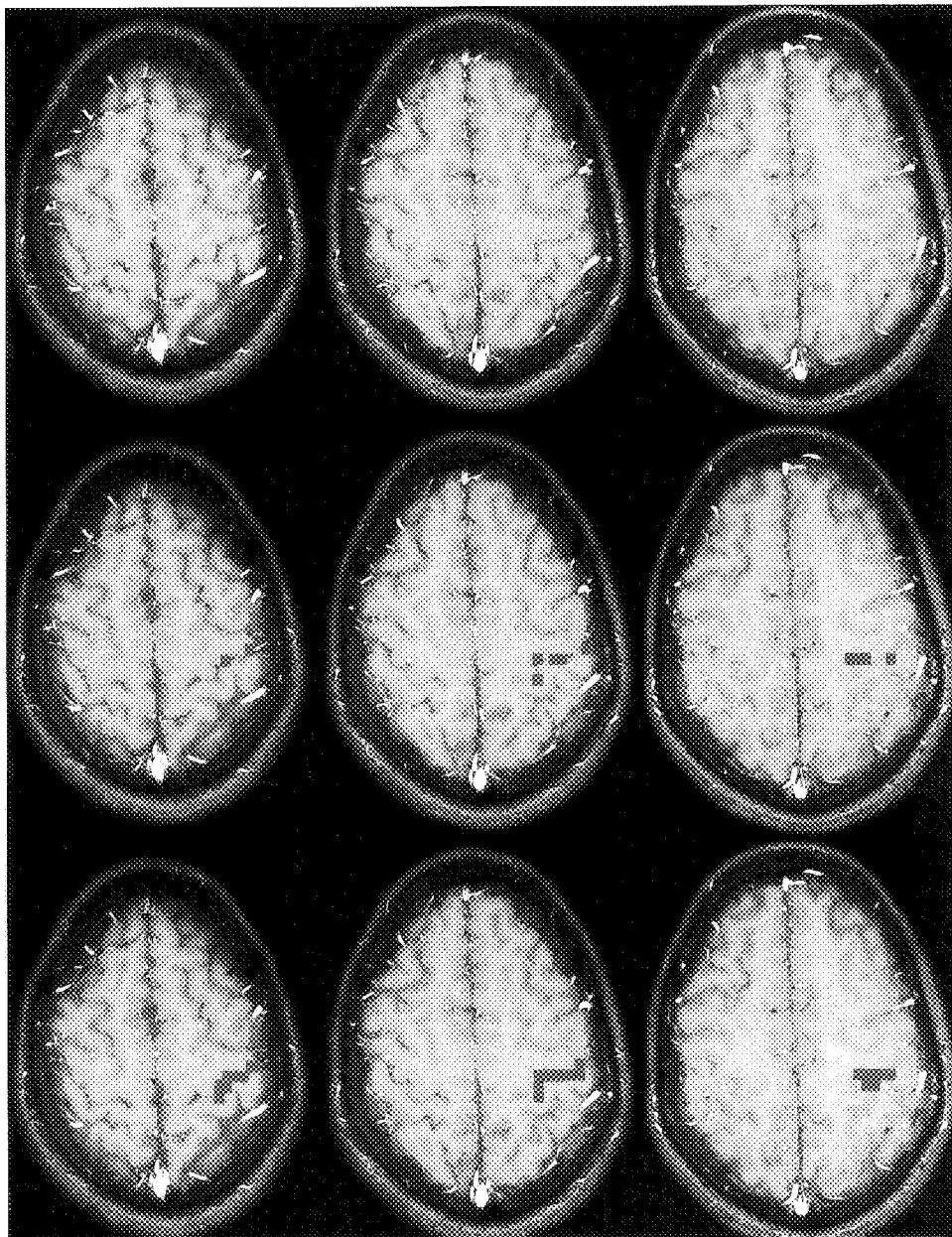


Figure 5. TOF images (top row) with overlays of the functional maps on these images acquired with SE L-EVI (middle row) and ASE L-EVI (bottom row) sequences.

Table 1
Comparison of Activation Studies in the Primary Sensorimotor Cortex using ASE and SE L-EVI Sequences

Volunteer	Number of Activated Voxels		Percentage of Voxels Overlapping Large Vessels (%)		Average Signal Change (%)	
	SE	ASE	SE	ASE	SE	ASE
1	6	18	.0	22.2	1.29	1.69
2	8	23	12.5	26.1	1.26	1.70
3	11	27	18.2	25.9	1.19	1.73
4	9	24	11.1	25.0	1.15	2.13
5	8	19	25.0	26.3	1.30	1.81
6	8	23	25.0	34.8	1.23	1.75
Mean	8.3	22.3	15.3	26.7	1.24	1.80
SD	1.6	3.3	9.6	4.2	.06	.17

the inversion pulse for the subsequent volume (eg, V_2 in Fig. 3b). This allows for reduction of signal instabilities generated by motion of the CSF. Images acquired with CSF nulling (TR = 1.4 seconds, assuming $T_1 = 2$ seconds for CSF) are shown in Figure 3a (bottom row).

All functional studies showed distinct activation-related signal changes in the contralateral primary senso-

rimotor cortex (PSM). Examples of the signal time courses in the activated contralateral PSM using the ASE and SE versions of the single-shot L-EVI sequence are shown in Figure 4. The signal change patterns are similar in the ASE and SE studies, but the mean amplitude is significantly larger in the ASE studies as compared with that in the SE studies ($P < .001$). Among the six normal vol-

unteers, signal increase in the activated voxels ranged from .80 to 4.40% (mean = 1.80% and SD = .17%) in the ASE studies and from .65 to 2.55% (mean = 1.24% and SD = .06%) in the SE studies.

Activated areas were examined for size and location by overlaying the activation maps onto the high-resolution TOF images. Figure 5 shows an example of the TOF images as well as the overlays of the activation maps on the TOF images. The number of voxels in the activated area and the percentage of activated voxels visibly overlapping large vessels in the ASE and SE studies are shown in Table 1. The mean number of activated voxels in the ASE studies was significantly larger than that in the SE studies of the six volunteers ($P < .00001$). The mean percentage of the activated voxels visibly overlapping large vessels in the ASE studies also was significantly larger than that in the SE studies ($P < .01$).

• DISCUSSION

Single-shot L-EVI allows for three-dimensional fMRI studies of human brain with high temporal resolution. Reasonable spatial resolution ($3.75 \times 5 \times 5 \text{ mm}^3$) was obtained by preselection of volume of interest. Increased volume coverage was demonstrated using a multivolume acquisition protocol.

The three-dimensional acquisition mode allowed for BOLD-sensitized imaging while suppressing origination from vascular structures, possibly remote from activated regions. Measured signal changes in experiments with strong inflow effects (eg, single-slice experiments performed under saturation conditions) exceed changes expected with BOLD contrast mechanisms, as demonstrated by earlier experiments (7,8). The magnitude of BOLD signal increases in the L-EVI studies (1.80% and 1.24% in the ASE and SE studies, respectively) were comparable to those of three-dimensional fast low-angle shot (FLASH) studies (11,18) and theoretical predictions (7), when corrected for differences in $T2^*$ weighting, suggesting that inflow effects were reduced in the L-EVI sequence.

In addition, the area of activation and the percent signal increases in the functional studies were larger in the ASE studies than in the SE studies. This is in agreement with earlier fMRI studies that showed that the $T2^*$ change is larger than $T2$ change during brain activation (21,22). Furthermore, the functional data illustrated that the activated regions detected by ASE sequence were more often visibly overlapping larger vessels, as determined from comparison with high-resolution TOF images. This observation also is in agreement with an earlier study showing that $T2^*$ -weighted sequences are relatively more sensitive to BOLD effects in and around larger vessels (in addition to the capillaries) as compared to $T2$ -weighted sequences, which are assumed to more selectively measure contributions from the capillary bed (21).

References

1. Ogawa S, Lee TM, Nayak AS, Glynn P. Oxygenation-sensitive contrast in magnetic resonance imaging of rodent brain at high magnetic field. *Magn Reson Med* 1990; 14:68-78.
2. Ogawa S, Lee TM, Ray AR, Tank DW. Brain magnetic resonance imaging with contrast dependent on blood oxygenation. *Proc Natl Acad Sci USA* 1990; 87:9868-9872.
3. Mansfield P. Multi-planar image formation using NMR spin echoes. *J Phys C* 1977; 10:L55-L58.
4. Kwong KK, Belliveau JW, Chesler DA, et al. Dynamic magnetic imaging of human brain activity during primary sensory stimulation. *Proc Natl Acad Sci USA* 1992; 89:5675-5679.
5. Bandettini PA, Wong EC, Hinks RS, Tikofsky RS, Hyde JS. Time course EPI of human brain function during task activation. *Magn Reson Med* 1992; 25:390-397.
6. Kwong KK. Functional magnetic resonance imaging with echo planar imaging. *Magn Reson Q* 1995; 11:1-20.
7. Boxerman JL, Bandettini PA, Kwong KK, et al. The intravascular contribution to fMRI signal change: Monte Carlo modeling and diffusion-weighted studies in vivo. *Magn Reson Med* 1995; 34:4-10.
8. Duyn JH, Moonen CTW, van Yperen GH, de Boer RW, Luyten PR. Inflow versus deoxyhemoglobin effects in "BOLD" functional MRI using gradient echoes at 1.5 T. *NMR Biomed* 1994; 7:83-88.
9. Gromiscek S, Beisteiner R, Hittmair K, Mueller E, Moser E. A possible role of in-flow effects in functional MR imaging. *Magn Reson Materials Phys Biol Med* 1993; 1:109-113.
10. Lai S, Hopkins AL, Haacke EM, et al. Identification of vascular structures as a major source of signal contrast in high resolution 2D and 3D functional activation imaging of motor cortex at 1.5 T: preliminary results. *Magn Reson Med* 1993; 30:387-392.
11. Duyn JH, Mattay VS, Sexton RH, et al. 3-Dimensional functional imaging of human brain using echo-shifted FLASH MRI. *Magn Reson Med* 1994; 32:150-155.
12. Mansfield P, Howseman AM, Ordidge RJ. Volumar imaging using NMR spin echoes: echo-volumar imaging (EVI) at 0.1 T. *J Phys E* 1989; 22:324-330.
13. Song AW, Wong EC, Hyde JS. Echo-volume imaging. *Magn Reson Med* 1995; 32:668-671.
14. Hykin J, Coxon R, Bowtell R, Glover P, Mansfield P. Temporal differences in functional activation between separate regions of the brain investigated with single shot echo volumar imaging at 3.0 T. In: Proceedings of the 3rd annual scientific meeting of the Society of Magnetic Resonance. Nice, France: Society of Magnetic Resonance, 1995; 1:451.
15. Unser M, Aldroubi A. A multiresolution image registration procedure using spline pyramids. In: Proceedings of the SPIE on Mathematical Imaging: Wavelet Applications in Signal and Image Processing. San Diego: SPIE, 1993; 2034:160-170.
16. Thevenaz P, Ruttimann UE, Unser M. Iterative multi-scale registration without landmarks. In: Proceedings of the International Conference on Image Processing, Washington, DC: (IEEE), 1995; 3:228-231.
17. Worsley K, Friston K. Analysis of fMRI time-series revisited: again. *Neuroimage* 1995; 2:173-181.
18. van Gelderen P, Ramsey N, Liu G, et al. Three-dimensional functional magnetic resonance imaging of human on a clinical 1.5-T scanner. *Proc Natl Acad Sci USA* 1995; 92:6906-6910.
19. Mattay VS, Frank JA, Santha AK, et al. Whole brain functional mapping with isotropic MRI. *Radiology* 1996; 201:399-404.
20. Zilles K. Cortex. In: Paxinos G, ed. The human nervous system. San Diego, Academic Press, Inc., 1990; 757-760.
21. Ogawa S, Menon RS, Tank DW, et al. Functional brain mapping by blood oxygenation level-dependent contrast magnetic resonance imaging. A comparison of signal characteristics with a biophysical model. *Biophys J* 1993; 64:803-812.
22. Bandettini PA, Wong EC, Jesmanowicz A, Hinks RS, Hyde JS. Spin-echo and gradient-echo EPI of human brain activation using BOLD contrast: a comparative study at 1.5 T. *NMR Biomed* 1994; 7:12-20.